# NUCLEAR DEFORMATION ENERGIES WITH THE WEIZSÄCKER–SKYRME MASS MODEL*

Ning Wang, Tao Li

Department of Physics, Guangxi Normal University, Guilin 541004, P.R. China
and
Guangxi Key Laboratory of Nuclear Physics and Technology
Guilin 541004, P.R. China

*(Received December 21, 2018)*

We use the Weizsäcker–Skyrme (WS) mass models to systematically investigate nuclear deformation energies. With an accuracy of 298 keV for the known masses, the WS4 mass model is quite helpful for exploring new magic numbers in neutron-rich region and nuclear deformation energies. We note that the predicted deformation energies of nuclei with the Hartree–Fock–Bogoliubov (HFB25) model are systematically larger than those with the WS models, especially for nuclei with sub-shell closures. The comparison of the deformation energies from the two models and the corresponding charge radii for nuclei with $N = 14$ are also presented.

DOI:10.5506/APhysPolBSupp.12.715

## 1. Introduction

As one of the basic quantities and inputs in nuclear physics, nuclear masses are very important not only in the study of nuclear physics, such as the synthesis of super-heavy nuclei (SHN) [1–3], fission [4, 5], nuclear symmetry energy, and so on, but also in the study of astrophysics, such as the r-process. Up to now, the masses of about 2500 nuclei have already been measured and those of about 4500 nuclei are still unknown. With great efforts, a number of nuclear mass models have been successfully proposed with a root-mean-square (r.m.s.) error of several hundred keV with respect to the known masses [6–11]. In addition to the mass measurement, the $\alpha$-decay energies $Q_\alpha$ of about 100 SHN have also been measured. These data are also helpful to test the available mass models and to study the structure of SHN [12–14].

* Presented at the XXV Nuclear Physics Workshop "Structure and Dynamics of Atomic Nuclei", Kazimierz Dolny, Poland, September 25–30, 2018.

As a macroscopic–microscopic mass model, the Weizsäcker–Skyrme (WS) model [9–11] was proposed, with considering the isospin dependence of model parameters and the mirror correction from the isospin symmetry. With the latest version (WS4) of the model [11], the 2353 measured masses in AME2012 [15] can be reproduced with an r.m.s. deviation of 298 keV. The WS models were largely tested by some groups. For example, Sobiczewski and Litvinov tested the accuracy of 12 different mass models with the data at different mass regions [16]. They concluded that *the WS3.3 model is the best of all 12 considered models*. Very recently, Sobiczewski and his collaborators re-tested these models with new data [17]. They concluded that *the best accuracy is obtained by WS3+RBF and WS4+RBF models*. RBF denotes the radial basis function correction [18, 19] which is a prominent global interpolation and extrapolation scheme to effectively describe the systematic errors of a global mass model. Very recently, the masses of $^{246}$Es, $^{251}$Fm, $^{249-252}$Md and $^{254}$No were directly measured in RIKEN [20]. After comparison of the predictions from five different models, the authors pointed that *particularly robust agreement is seen with the WS4$^{RBF}$ mass model*.

In addition to the isospin dependence of model parameters and isospin symmetry in the WS models, the consideration of the influence of nuclear deformations on the macroscopic energy is different from other macroscopic–microscopic mass models. In the WS models, the deformation factor in the liquid-drop energy is directly expressed as an analytical formula under the parabolic approximation for small deformations, which is inspired by the Skyrme energy density functional together with the extended Thomas–Fermi approach. The parabolic approximation for deformation factor could significantly affect the predictions of nuclear deformations at ground states. Nuclear deformations have direct relationship with nuclear r.m.s. charge radii and are usually used as a probe to explore the appearance of magicity in nuclei. It is, therefore, interesting to systematically investigate the nuclear deformation energies with this model.

## 2. Deformation factor in the macroscopic energies

In this section, we introduce two nuclear mass models: the Myers–Swiatecki liquid-drop (MS-LD) model [4] and the WS model for the description of nuclear deformation energies. Here, we focus on the deformation dependence of potential energies in nuclei around their ground states.

### *2.1. Myers–Swiatecki liquid drop model*

In the semi-empirical nuclear mass formula proposed by Myers and Swiatecki, the liquid-drop energy of a nucleus is written as [4]

$$\begin{aligned} E_{\mathrm{MS-LD}}(A,Z,\mathrm{shape}) &= -15.667A\left(1-1.79I^2\right) \\ &\quad +18.56A^{2/3}\left(1-1.79I^2\right)f(\mathrm{shape}) \\ &\quad -1.211\frac{Z^2}{A}+0.717\frac{Z^2}{A^{1/3}}g(\mathrm{shape})\,. \end{aligned} \tag{1}$$

The forms of the deformation factor $f$ in the surface energy and $g$ in the Coulomb energy are very complicated for a realistic nuclear system. For a distorted sphere with small quadrupole deformations, the factors $f$ and $g$ can be approximately (to second order) expressed as $f(\beta_2) \approx 1+\beta_2^2/(2\pi)$ and $g(\beta_2) \approx 1-\beta_2^2/(4\pi)$, respectively [22].

In Fig. 1, we show the calculated macroscopic energies of $^{16}$O and $^{48}$Ca from the MS-LD model. Here, the results from the Skyrme energy density functional together with the extended Thomas–Fermi approach (ETF2) including all terms up to second order in the spatial derivatives [23, 24] are also presented for comparison. One can see from Fig. 1 that the macroscopic energy of a nucleus varies with the quadrupole deformations as a parabolic behavior in general for small deformations, and the curvatures from the two approaches are close to each other.

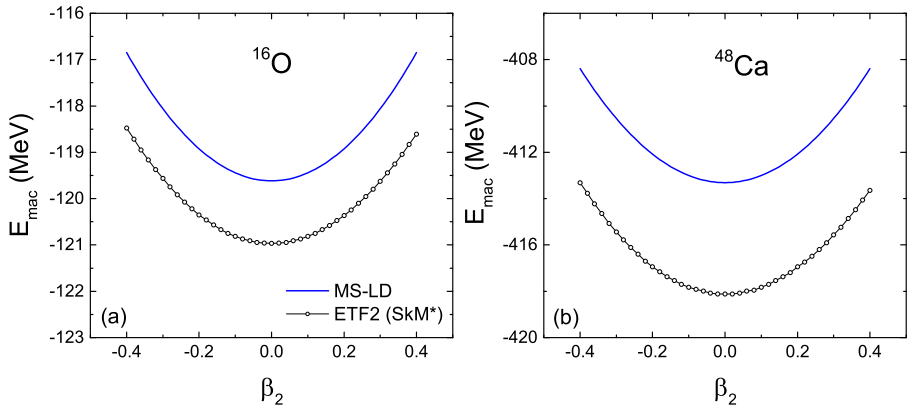


Fig. 1. Macroscopic energies of $^{16}$O and $^{48}$Ca. The solid curves denote the results of MS-LD model together with the formulas for $f$ and $g$ in the text. The circles denote the results from the ETF2 approach with SkM*.

### 2.2. Weizsäcker–Skyrme mass model

In the WS model, the total energy of a nucleus is written as a sum of the liquid-drop energy, the Strutinsky shell correction $\Delta E$ and the residual correction $\Delta_{\rm res}$,

$$E(A,Z,\beta) = E_{\rm LD}(A,Z)\prod_{k\geq 2}\left(1+b_k\beta_k^2\right) + \Delta E(A,Z,\beta) + \Delta_{\rm res}\,. \qquad (2)$$

The liquid-drop energy of a spherical nucleus $E_{\rm LD}(A,Z)$ is described by a modified Bethe–Weizsäcker mass formula

$$E_{\rm LD}(A,Z) = a_{\rm v}A + a_{\rm s}A^{2/3} + E_{\rm C} + a_{\rm sym}I^2A + a_{\rm pair}A^{-1/3}\delta_{np} \qquad (3)$$

with the isospin asymmetry $I=(N-Z)/A$ and the Coulomb energy $E_{\rm C}$.

The deformation factor $\prod(1+b_k\beta_k^2)$ in the WS model is directly expressed as an analytical formula under the parabolic approximation for small deformations. Here, we would like to emphasize that the total macroscopic potential energy is assumed to be a parabolic shape, which does not mean the same deformation factor for each term in Eq. (3). The mass dependence of the curvatures $b_k$ in Eq. (2) is written as [9]

$$b_k = \left(\frac{k}{2}\right)g_1A^{1/3} + \left(\frac{k}{2}\right)^2 g_2A^{-1/3}\,, \qquad (4)$$

which significantly reduces the computation time for the calculation of deformed nuclei.

### 2.3. Mass dependence of the curvatures

In Fig. 2, we show the calculated curvatures of the macroscopic potential energies around small deformations for nuclei along the $\beta$-stability line. We note that the absolute values of the curvatures decrease with masses and gradually approach zero for SHN, which results in the disappearance of the macroscopic fission barrier of SHN. In addition, the obtained curvatures with the MS-LD model together with the formulas for $f$ and $g$ in the text are slightly smaller than the results from the ETF2 approach. The results of the WS4 model [11] (with $g_1=0.01046$ and $g_2=-0.5069$) are obviously smaller than those of two other models at light and intermediate mass region, which implies that one obtains a relatively smaller nuclear deformations for light nuclei with the WS4 model.

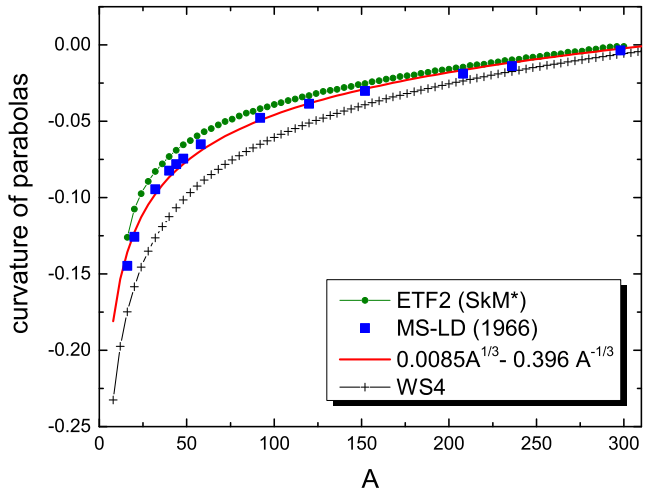


Fig. 2. Curvatures $b_k$ in the macroscopic energies for nuclei along the $\beta$-stability line. The circles, the squares and the crosses denote the results from ETF2, MS-LD and WS4, respectively. The solid curve denotes a fit to the squares.

## 3. Deformation energies of nuclei

The deformation energy is defined as the difference in energy of a nucleus between its spherical and equilibrium shapes [3], *i.e.*,

$$E_{\rm def} = E(0) - E(\beta_{\rm gs})\,. \tag{5}$$

Thus, this quantity is the gain in energy of a nucleus due to its deformation.

### *3.1. $E_{def}$ of nuclei along the $\beta$-stability line*

In Fig. 3, we show the predicted deformation energies of nuclei along the $\beta$-stability line with three different mass models: WS*, WS4 and HFB25. Here, the $\beta$-stability line is described by Green's formula. Nuclear deformations $\beta_2$, $\beta_4$ and $\beta_6$ are considered in the WS calculations. The macroscopic potential energy has a minimum at spherical shape according to the parabolic approximation. Together with the Strutinsky shell correction from the axially deformed Woods–Saxon potential [21] and the residual corrections, one obtains the ground-state shapes for a certain nucleus. The results with the WS* model are very close to those with the WS4 model, due to the same theoretical framework. For nuclei with the known magic numbers, one can see an evident decrease in the deformation energies. In addition to the known magic numbers, we note that the deformation energies of nuclei with

$N = 16$, 32, 40, 64 are also evidently smaller than those of their neighboring nuclei. Some studies [25–28] indicate that $N = 14$, 16, 32 could be magic numbers in neutron-rich region, which is helpful to further test and improve nuclear mass models. The results of the HFB25 model are systematically larger than those of WS* and WS4 models, especially for light and intermediate nuclei, which could be due to the different deformation factors adopted in the models.

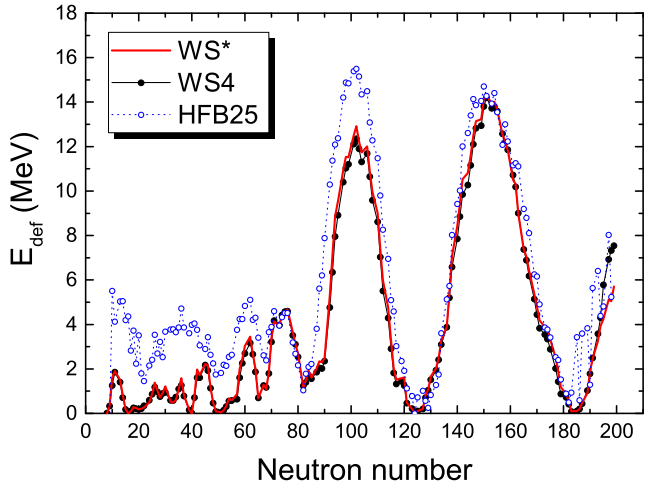


Fig. 3. Deformation energies of nuclei along the $\beta$-stability line. The solid curve, the filled circles and the open circles denote the results from the WS* model, the WS4 model and the HFB25 model, respectively.

### *3.2. $E_{def}$ of nuclei along the shell stability line*

According to the calculations of the WS model, it is interesting to note that a number of nuclei with relatively larger shell corrections (in absolute value) locate along the line $N = 1.37Z+13.5$ which is called the shell stability line (SSL) [10, 29]. In Fig. 4, we show the contour plot of the calculated shell corrections from the WS4 model for nuclei over the whole nuclear chart. In addition to the known doubly-magic nuclei, the shell corrections for $^{46}$Si and $^{78}$Ni are also evidently large. The experimental investigation on the single-neutron states in $^{79}$Zn at CERN supports the picture of a robust $N = 50$ shell closure for $^{78}$Ni [30]. For $^{46}$Si, the neutron number $N = 32$ could be new magic number, considering the measured large shell gap in $^{52}$Ca [27]. For SHN with $Z = 120$, there are two minima for the $\alpha$-decay energies [29]: $Q_\alpha = 12.98$ MeV at $N = 178$ which locates at the SSL and $Q_\alpha = 12.74$ MeV at $N = 184$. The neutron number in the synthesized SHN $^{294}$Og [31] is

very close to the position of $N = 178$. It is, therefore, quite interesting and important to produce more neutron-rich SHN such as $^{296}$Og and $^{297}$Og to explore the trend of $Q_\alpha$.

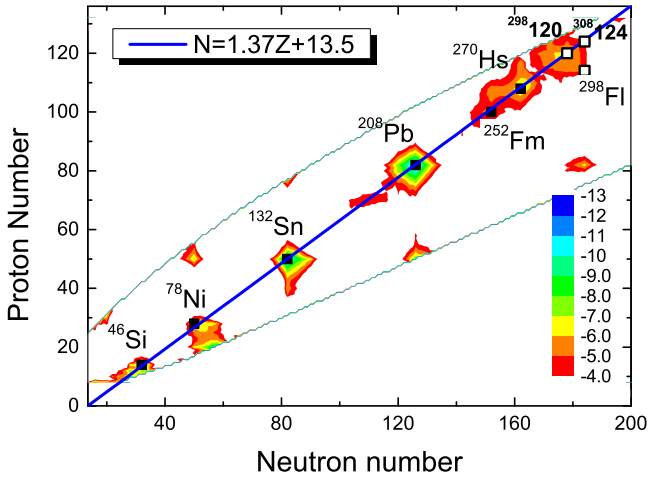


Fig. 4. Predicted shell corrections with the WS4 mass model.

In addition to the shell corrections, it is also interesting to study the deformation energies of nuclei along the SSL. In Fig. 5, we show the calculated $E_{\rm def}$ with the three models. For intermediate nuclei with $N \leq 82$, the results from the three models are relatively close to each other. For lanthanides and SHN around $N = 170$, the predicted deformation energies with the HFB25 model are obviously larger than the WS calculations.

### *3.3. $E_{def}$ and charge radii of nuclei with $N = 14$*

To further understand the discrepancies of the predicted deformation energies, we systematically compare the results from WS* and HFB27. We note that the predicted deformations for nuclei with sub-shell closure such as $N = 14$ and $Z = 64$ are quite different from these two models. As an example, we show in Fig. 6 (a) the deformation energies of nuclei with $N = 14$. The results with the WS* model are significantly smaller than those with HFB25, since the calculated shapes for these nuclei at their ground states are nearly spherical from the WS* model, whereas well-deformed shapes are predicted for these nuclei from the HFB25 model.

Due to the difficulties to directly measure the deformation energies of nuclei, it is, therefore, necessary to determine the shapes of these nuclei from other quantities. It is known that nuclear r.m.s. charge radii are directly related to nuclear shapes. Considering the quadrupole $\beta_2$ and hexadecapole

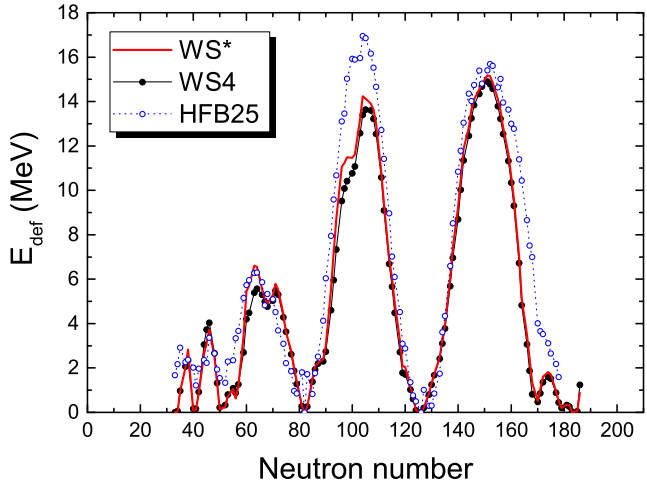


Fig. 5. The same as Fig. 3 but for nuclei along the line $N = 1.37Z + 13.5$.

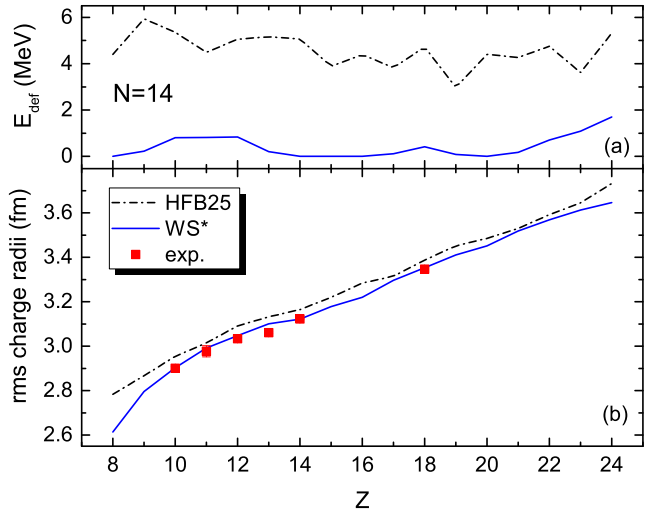


Fig. 6. Deformation energies (a) and r.m.s. charge radii (b) for nuclei with $N = 14$. The dashed and the solid curves denote the results from the HFB25 model and the WS* model, respectively. The squares denote the data from [33].

$\beta_4$ deformations of nuclei, the r.m.s. charge radius $r_{\rm ch}$ of a nucleus can be approximately written as [32]

$$r_{\rm ch} = \langle r^2 \rangle^{1/2} \simeq \sqrt{\frac{3}{5}} R_{\rm c} \left[ 1 + \frac{5}{8\pi} \left( \beta_2^2 + \beta_4^2 \right) \right] . \tag{6}$$

The increase of nuclear deformations should cause an increase of nuclear r.m.s. charge radius. In Fig. 6 (b), we show the corresponding r.m.s. charge radii of these nuclei. The solid curve denote the WS* calculations [32], *i.e.* with $R_c = 1.226A^{1/3} + 2.86A^{-2/3} - 1.09(I - I^2) + 0.99\Delta E$ together with the shell corrections $\Delta E$ and nuclear deformations from the WS* mass model. The experimental data [33] can be well reproduced with the WS* calculations. The predictions from the HFB25 are systematically larger than the data, which might be due to the over-predicted nuclear deformations.

## 4. Summary and discussions

With the parabolic approximation for the deformation factor in the macroscopic potential energy, the mirror constraint for the Strutinsky shell corrections and some residual corrections, the Weizsäcker–Skyrme (WS4) mass model can reproduce the 2353 known masses with an r.m.s. deviation of 298 keV. The tests for the WS models from some groups support its good predictive power. With this model, we systematically investigate the deformation energies of nuclei. In addition to the known magic numbers, we find that the deformation energies of nuclei with $N = 16$, 32, 40, 64 are also evidently smaller than those of their neighbouring nuclei. We also note that the predicted deformation energies of nuclei with the Hartree–Fock–Bogoliubov (HFB25) model are systematically larger than those with the WS models, especially for nuclei with sub-shell closures. It is probably due to that: (1) the curvatures of the deformation factor in the WS4 model are obviously smaller than those of HFB25 at light and intermediate mass region, and (2) the nuclear deformations for some nuclei with sub-shell closures such as $N = 14$ might be over-predicted in the HFB25 calculations.

Obviously, the parabolic approximation for the deformation factor adopted in the present versions of the WS models is not applicable in the study of the potential energy surface along nuclear fission path in which the extremely large deformations of nuclear system are involved. To extend the WS models for description of nuclear large deformations, the higher order terms in the deformation factor should be further considered.

One of the authors (N.W.) is grateful to Prof. Adam Sobiczewski for his great encouragement and his help to the WS mass models. This work was supported by the National Natural Science Foundation of China (Nos. U1867212, 11422548, 11747307), the Guangxi Natural Science Foundation (No. 2015GXNSFDA139004), and the Foundation of Guangxi innovative team (Nos. 2017GXNSFGA198001, 2016GXNSFFA380001). The WS mass tables are available at: http://www.imqmd.com/mass/

## REFERENCES


[1] Yu.Ts. Oganessian *et al.*, *Phys. Rev. Lett.* **104**, 142502 (2010).
[2] S. Ćwiok, P.H. Heenen, W. Nazarewicz, *Nature* **433**, 705 (2005).
[3] A. Sobiczewski, K. Pomorski, *Prog. Part. Nucl. Phys.* **58**, 292 (2007).
[4] W.D. Myers, W.J. Swiatecki, *Nucl. Phys.* **81**, 1 (1966).
[5] B.N. Lu, E.G. Zhao, S.G. Zhou, *Phys. Rev. C* **85**, 011301(R) (2012).
[6] D. Lunney, J.M. Pearson, C. Thibault, *Rev. Mod. Phys.* **75**, 1021 (2003).
[7] S. Goriely, N. Chamel, J.M. Pearson, *Phys. Rev. C* **88**, 024308 (2013).
[8] J. Duflo, A.P. Zuker, *Phys. Rev. C* **52**, 23 (1995).
[9] N. Wang, M. Liu, X.Z. Wu, *Phys. Rev. C* **81**, 044322 (2010).
[10] N. Wang, Z.Y. Liang, M. Liu, X.Z. Wu, *Phys. Rev. C* **82**, 044304 (2010).
[11] N. Wang, M. Liu, X.Z. Wu, J. Meng, *Phys. Lett. B* **734**, 215 (2014).
[12] Yu.Ts. Oganessian, V.K. Utyonkov, *Nucl. Phys. A* **944**, 62 (2015).
[13] Y.Z. Wang *et al.*, *Phys. Rev. C* **92**, 064301 (2015).
[14] A. Sobiczewski, *J. Phys. G: Nucl. Part. Phys.* **43**, 095106 (2016).
[15] G. Audi *et al.*, *Chin. Phys. C* **36**, 1287 (2012).
[16] A. Sobiczewski, Y.A. Litvinov, *Phys. Scr.* **T154**, 014001 (2013); *Phys. Rev. C* **89**, 024311 (2014).
[17] A. Sobiczewski, Y.A. Litvinov, M. Palczewski, *At. Data Nucl. Data Tables* **119**, 1 (2018).
[18] N. Wang, M. Liu, *Phys. Rev. C* **84**, 051303(R) (2011).
[19] Z.M. Niu *et al.*, *Phys. Rev. C* **88**, 024325 (2013).
[20] Y. Ito *et al.*, *Phys. Rev. Lett.* **120**, 152501 (2018).
[21] S. Ćwiok *et al.*, *Comput. Phys. Commun.* **46**, 379 (1987).
[22] W. Greiner, J.A. Maruhn, *Nuclear Models*, Springer-Verlag, Berlin Heidelberg 1996.
[23] J. Bartel, K. Bencheikh, *Eur. Phys. J. A* **14**, 179 (2002).
[24] M. Liu *et al.*, *Nucl. Phys. A* **768**, 80 (2006).
[25] C.R. Hoffman *et al.*, *Phys. Lett. B* **672**, 17 (2009).
[26] I. Angeli, K.P. Marinova, *J. Phys. G: Nucl. Part. Phys.* **42**, 055108 (2015).
[27] F. Wienholtz *et al.*, *Nature* **498**, 346 (2013).
[28] N. Wang, M. Liu, *Chin. Sci. Bull.* **60**, 1145 (2015).
[29] N. Wang, M. Liu, X.Z. Wu, J. Meng, *Phys. Rev. C* **93**, 014302 (2016).
[30] R. Orlandi *et al.*, *Phys. Lett. B* **740**, 298 (2015).
[31] Yu.Ts. Oganessian *et al.*, *Phys. Rev. C* **74**, 044602 (2006).
[32] N. Wang, T. Li, *Phys. Rev. C* **88**, 011301(R) (2013).
[33] I. Angeli, K.P. Marinova, *At. Data Nucl. Data Tables* **99**, 69 (2013).